Available online at www.sciencedirect.com

ELSEVIER

Procedia Chemistry 1 (2009) 1323–1326

Procedia Chemistry

www.elsevier.com/locate/procedia

Proceedings of the Eurosensors XXIII conference

Sensor Fusion Algorithm and Calibration for a Gyroscope-free IMU

P. Schopp[a]*, L. Klingbeil[b], C. Peters[a,b], A. Buhmann[a], Y. Manoli[a,b]

[a]*Chair of Microelectronics, University of Freiburg - IMTEK, 79110 Freiburg, Germany*
[b]*HSG-IMIT, 78052 Villingen-Schwenningen, Germany*

Abstract

This paper presents a gyroscope-free inertial measurement unit (IMU) that only consists of linear acceleration sensors. Only a simple matrix multiplication has to be performed in order to calculate the complete relative movement of a body. However, the precise positions and orientations of the sensors within the body frame have to be known in order to calculate the exact movement of the body. A simple and effective calibration algorithm developed in this paper can be applied to determine these parameters entirely even without any previous knowledge. Measurements on a 3D-rotation table were carried out to demonstrate the accuracy improvements after the calibration. Thereby, the RMS error of the angular rate was reduced by a factor of 2.8.

Keywords: Sensor Fusion; Gyroscope-free IMU; Kalman Filter; Calibration

1. Introduction

A conventional IMU comprises three gyroscopes and three accelerometers. However, gyroscopes are afflicted with certain drawbacks in their characteristics i.e. bias drift, shock resistance, durability[1]. In contrast to this, a gyroscope-free IMU (GF-IMU) senses the complete relative body movement only by accelerometers. Thereby, the GF-IMU concept is motivated by two concerns. It intends to first overcome the mentioned disadvantages of gyroscopes and second, to reduce the total system cost by using already existing accelerometers as for example in a car[2].

At least six accelerometers are necessary to completely determine the relative motion of a body[3]. However, this minimum number of accelerometers is only feasible in a certain cube configuration of the sensors[3]. Furthermore, using six sensors only the angular and the transversal acceleration can be detected. The angular velocity has to be computed via an integration step, which leads to drift errors. Our approach, using 12 sensors, makes it possible to determine the angular rate directly and also permits a nearly arbitrary placement of the sensors[4]. But, with a GF-IMU it is not possible to directly calculate the sign of the angular movement. To overcome this drawback, an Unscented Kalman Filter (UKF) is applied to merge the information of the angular acceleration and the angular rate and thus robustly estimate the sign of the body's rotation[5].

For an exact computation of the body motion the positions and sensitive axes as well as the signal offset of the accelerometers have to be known. This paper provides an effective calibration algorithm for determining these parameters using reference measurements and values delivered by the accelerometers.

* Patrick Schopp. Tel.: +49-(0)761-203-7458; fax: +49-(0)761-203-7592.
E-mail address: Patrick.Schopp@imtek.uni-freiburg.de.

doi:10.1016/j.proche.2009.07.330

$$\boldsymbol{y} = \begin{bmatrix} a_{S1} \\ a_{S2} \\ a_{S3} \\ a_{S4} \\ a_{S5} \\ a_{S6} \\ a_{S7} \\ a_{S8} \\ a_{S9} \\ a_{S10} \\ a_{S11} \\ a_{S12} \end{bmatrix} = A \begin{bmatrix} a_{B,x} \\ a_{B,y} \\ a_{B,z} \\ \dot{\omega}_{B,x} \\ \dot{\omega}_{B,y} \\ \dot{\omega}_{B,z} \\ \omega^2_{B,x} \\ \omega^2_{B,y} \\ \omega^2_{B,z} \\ \omega_{B,x}\omega_{B,y} \\ \omega_{B,x}\omega_{B,z} \\ \omega_{B,y}\omega_{B,z} \end{bmatrix} + \begin{bmatrix} a_{oS1} \\ a_{oS2} \\ a_{oS3} \\ a_{oS4} \\ a_{oS5} \\ a_{oS6} \\ a_{oS7} \\ a_{oS8} \\ a_{oS9} \\ a_{oS10} \\ a_{oS11} \\ a_{oS12} \end{bmatrix} = A\boldsymbol{z} + \boldsymbol{a_o}$$

Equation 2.

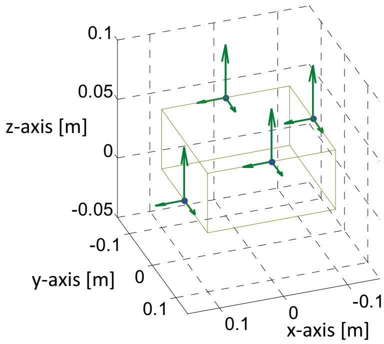

Fig. 1. Possible sensor configuration. The sensors are grouped into three axial accelerometers. The arrows represent their sensitive axes.

2. System equations

Considering an accelerometer S fixed within a rigid body B the measured acceleration a_S of sensor S can be calculated using the following equation:

$$a_S = \boldsymbol{s}^T(\boldsymbol{a}_B + \dot{\boldsymbol{\omega}}_B \times \boldsymbol{r} + \boldsymbol{\omega}_B \times (\boldsymbol{\omega}_B \times \boldsymbol{r})) + a_o \quad (1)$$

Thereby, the relative movement of the body is described by the acceleration of the body $\boldsymbol{a}_B$, the angular velocity $\boldsymbol{\omega}_B$, and the angular acceleration $\dot{\boldsymbol{\omega}}_B$. The time invariant parameters within Equation 1 are the sensor's sensitive axis $\boldsymbol{s}$, its position $\boldsymbol{r}$ with respect to the body frame, and its signal offset a_o. By incorporating 12 sensors a linear set of equations can be constructed (Equation 2). The resulting 12x12 parameter matrix A contains only information about the positions $\boldsymbol{r}$ and the sensitive axes $\boldsymbol{s}$ of the sensors. All information about the relative body motion is given in vector $\boldsymbol{z}$. By inverting A it is possible to calculate $\boldsymbol{z}$ for a given measurement vector $\boldsymbol{y}$ applying:

$$\boldsymbol{z} = A^{-1}(\boldsymbol{y} - \boldsymbol{a_o}) \quad (3)$$

This leads to the only requirement for the configuration of the sensors: matrix A must be invertible. This is the case, if the row vectors of A are linearly independent. Therefore, a valid sensor configuration can be found by applying a simple rule of thumb: If the sensors are clustered into sensor nodes of three sensors each, then the sensitive axes within one sensor node have to be linearly independent and the positions of the sensor nodes may not be coplanar. Fig. 1 shows such a possible sensor configuration. The geometrical dimension is the same as the one used for the experimental setup. A more detailed version of the derivation of Equation 2 can be found in [5].

3. Unscented Kalman Filter

Vector $\boldsymbol{z}$ of Equation 2 incorporates the angular velocity $\boldsymbol{\omega}_B$ in a quadratic form. Thus, the sign of $\boldsymbol{\omega}_B$, which represents the direction of the rotation, is lost. The recursive predictor-corrector structure of the UKF (Fig. 2) is capable to estimate the sign of $\boldsymbol{\omega}_B$. This section focuses on the models employed for the GF-IMU. A good explanation of the UKF framework can be found in [6].

The state $\boldsymbol{x}$ at time step k of the GF-IMU is defined as $\boldsymbol{x}_k = [\boldsymbol{a}_{B,k} \quad \boldsymbol{\omega}_{B,k} \quad \dot{\boldsymbol{\omega}}_{B,k}]^T$. The process model f predicts the state of the system at time step k based on the previous system state $\boldsymbol{x}_{k-1}$. It has to fulfill the form $\boldsymbol{x}_k = f(\boldsymbol{x}_{k-1}, \boldsymbol{v}_{k-1})$, where $\boldsymbol{v}_{k-1}$ is the process noise. The following equations were applied as the process model:

$$\begin{aligned} \boldsymbol{a}_{B,k} &= \boldsymbol{a}_{B,k-1} + \boldsymbol{v}_{a_B} \\ \boldsymbol{\omega}_{B,k} &= \boldsymbol{\omega}_{B,k-1} + (\dot{\boldsymbol{\omega}}_{B,k-1} + \boldsymbol{v}_{\dot{\boldsymbol{\omega}}_B})dT \\ \dot{\boldsymbol{\omega}}_{B,k} &= (\dot{\boldsymbol{\omega}}_{B,k-1} + \boldsymbol{v}_{\dot{\boldsymbol{\omega}}_B}) \end{aligned} \quad (4)$$

In this model it is assumed that there is no change in the body acceleration and in the angular acceleration between two time steps. Thus, the process noise $\boldsymbol{v}$ must provide for the fact that a change of acceleration can actually occur. The time step dT is determined by the sampling rate, which is 250Hz for the experiments presented here.

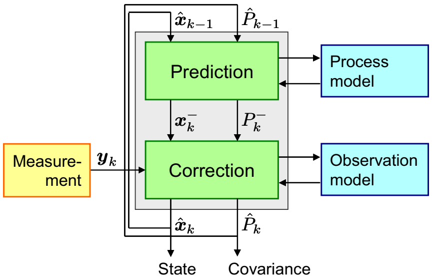

Fig. 2. The UKF framework. $\hat{\boldsymbol{x}}$ and $\hat{P}$ denote the estimated state and its covariance. $\boldsymbol{x}^-$and P^- are their respective predictions.

Fig. 3. The gyroscope-free IMU on the 3D rotation table.

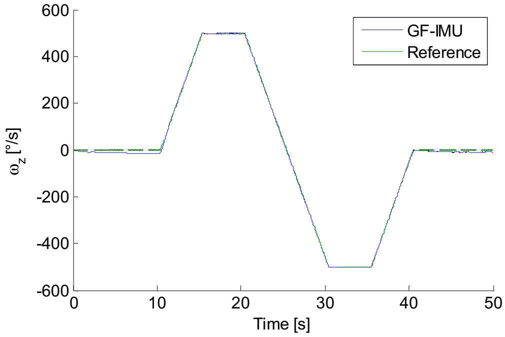

Fig. 4. Filter results of ω_z for a rotation around the body's z-axis. The GF-IMU was calibrated beforehand.

The predicted measurement is calculated by the observation model h based on the predicted state $\boldsymbol{x}^-$. It follows the form $\boldsymbol{y}_k = h(\boldsymbol{x}_k, \boldsymbol{n}_k)$, where $\boldsymbol{n}_k$ is the observation noise. For the GF-IMU, $\boldsymbol{n}_k$ is the standard deviation of the 12 accelerometers collected in a 12 by 1 vector and is assumed to be time invariant. Equation 2 is the main part of the observation model of the GF-IMU. However, the quadratic terms of vector z have to be calculated before applying Equation 2. Within the observation model Equation 2 is expanded to: $\boldsymbol{y}_k = A\boldsymbol{z}_k + \boldsymbol{a_o} + \boldsymbol{n}_k$.

The conjunction of process and observation model provides that the angular velocity $\boldsymbol{\omega}_B$ is updated both by the quadratic terms of z, resulting from the centrifugal force, and at the same time by the integration of $\dot{\boldsymbol{\omega}}_B$, which derives from the tangential force. This combination prevents drift errors and enables a stable estimation of the sign of $\boldsymbol{\omega}_B$. To investigate the estimation of the sign of the angular rate and the prevention of drift errors a simple rotation about the GF-IMU's z-axis was performed by a 3D rotation table (Fig. 3). The built in incremental decoders of the table provide enough accuracy to serve as a reference. A graph of the filter results is provided in Fig. 4.

4. Calibration

The accuracy of the filter results depend on the precise knowledge of the accelerometer parameters collected in matrix A and the offset vector $\boldsymbol{a_o}$. For example, if the assumed sensitive axis of a sensor differs from the actual sensitive axis of the real life set up, incorrect detections of $\dot{\boldsymbol{\omega}}_B$ appear in the filter results (Fig. 5a). Using the calibration scheme presented in this paper, the entire parameters of the real life set up can be identified. Measurements from the GF-IMU and reference states form the basis of the parameter construction. In order to join matrix A and the offset vector $\boldsymbol{a_o}$ Equation 2 can be reformulated to:

$$\boldsymbol{y} = \begin{bmatrix} A & \boldsymbol{a_o} \end{bmatrix} \begin{bmatrix} \boldsymbol{z} \\ 1 \end{bmatrix} \tag{5}$$

To build an over determined system this equation is expanded for n measurements and n corresponding reference states:

$$\begin{bmatrix} \boldsymbol{y}_1 & \dots & \boldsymbol{y}_n \end{bmatrix} = \begin{bmatrix} A & \boldsymbol{a_o} \end{bmatrix} \begin{bmatrix} \boldsymbol{z}_1 & \dots & \boldsymbol{z}_n \\ 1 & \dots & 1 \end{bmatrix} \tag{6}$$

This set of equations can be solved for the common parameter matrix $[A \quad \boldsymbol{a_o}]$ by calculating the Moore–Penrose pseudoinverse of the matrix that holds the reference states:

$$\begin{bmatrix} A & \boldsymbol{a_o} \end{bmatrix} = \begin{bmatrix} \boldsymbol{y}_1 & \dots & \boldsymbol{y}_n \end{bmatrix} \begin{bmatrix} \boldsymbol{z}_1 & \dots & \boldsymbol{z}_n \\ 1 & \dots & 1 \end{bmatrix}^+ \tag{7}$$

This equation is a solution in a least square sense for the over determined system. Since Equation 2 is a linear set of equations, at least 2 different values for each entry of the state vector z have to be imposed on the GF-IMU in a calibration run. For the calibration presented here, an overlay of all rotational freedoms of the 3D rotation table was used as the calibration run. The samples were taken for 2 min at 250 Hz.

Fig. 6 shows a comparison of the positions of the sensors as given in the construction plan and as determined by the calibration. The accuracy of the filter results is evaluated for the rotation around the body's z-axis shown in

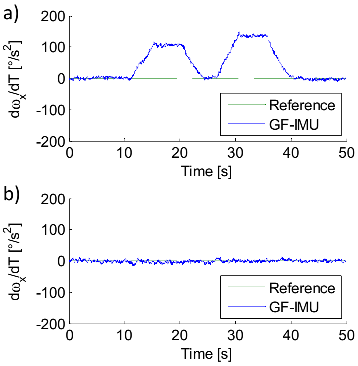

Fig. 5. Measured angular acceleration $\dot{\omega}_{B,x}$ detected for the rotation around the body's z-axis with a) offset adjustment and parameters based on the construction plan and b) after calibration.

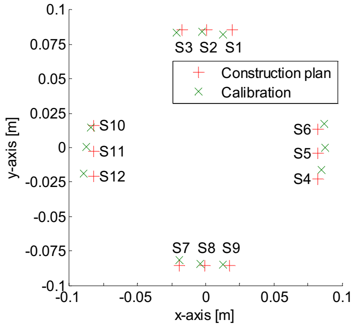

Fig. 6. The x-y positions of the 12 sensors (S1…S12) given in the construction plan and as determined by the calibration.

RMS Error:		Construction plan based	After calibration	Ideal Simulation
Body acceleration [m/s²] $\boldsymbol{a}_B$	x	0.14	0.03	0.02
	y	0.05	0.02	0.02
	z	0.07	0.05	0.02
Angular velocity [°/s] $\boldsymbol{\omega}_B$	x	17.75	8.53	1.18
	y	17.08	9.94	1.10
	z	18.17	6.54	0.92
Angular acceleration [°/s²] $\dot{\boldsymbol{\omega}}_B$	x	67.80	4.03	2.37
	y	30.07	4.18	2.12
	z	29.67	13.20	12.13

Tab. 1. Measured RMS error of the GF-IMU evaluated with offset adjusted sensor signals and parameters based on the construction plan, as well as after calibration. The simulation is based on ideal sensor position and orientation parameters.

Fig.4. The RMS error of the state variables is concluded in Tab. 1. The accuracy of the IMU after calibration is compared to the results using positions and orientations given in the construction plan and to a simulation based on ideal parameters. For the evaluation based on the construction plan, a simple offset adjustment of the sensor signals has been applied, since this is a standard calibration procedure. The largest improvement can be noticed for the angular acceleration, since its incorrect detections are compensated (Fig. 5b). The remaining differences of the RMS error to the ideal simulation are caused by the imperfection of the applied model (Equation 1). Sensor characteristics as the non-linearity and the cross sensitivity are not considered in this model.

5. Conclusion

This work presents a gyroscope-free IMU that only employs linear acceleration sensors. Using the calibration scheme presented in this paper the entire parameters of the GF-IMU can be determined without previous knowledge. Thus, an arbitrary placement of the sensors is feasible. At the same time, the accuracy of the filter results can be improved.

Acknowledgements

This work is supported by the German Research Foundation (DFG) under Grant Number GR1103.

References

1. N. Yazdi, F. Ayazi, K. Najafi, "Micromachined Inertial Sensors", *Proceedings of the IEEE*, 1998, vol. 86, pp. 1640-1659.
2. H. Weinberg, "MEMS Sensors are Driving the Automotive Industry", *Sensors*, 2002, vol. 19, pp. 36-41.
3. C. Tan, S. Park, "Design of accelerometer-based inertial navigation systems", *IEEE Transactions on Instrumentation and Measurement*, 2005, vol. 54, pp. 2520-2530.
4. C. Peters, A. Buhmann, D. Maurath, Y. Manoli, "A novel Full Accelerometer Based Inertial Navigation System", *Proceedings Mikrosystemtechnik Kongress*, 2005, pp. 233-236.
5. A. Buhmann, C. Peters, M. Cornils, Y. Manoli, "A GPS aided Full Linear Accelerometer Based Gyro-scope-free Navigation System", *Proceedings IEEE/ION PLANS*, 2006, pp. 622-629.
6. E. Wan, R. Van Der Merwe, "The Unscented Kalman Filter for Nonlinear Estimation", *Proceedings of the IEEE 2000 Adaptive Systems for Signal Processing, Communications, and Control Symposium*, 2000, pp. 153-158